Scholars LITERATURE

La Prensa Medica Argentina

Research Article

DOI: https://doi.org/10.47275/0032-745X-225
Volume 106 Issue 4

Postnatal Changes of Lung Structure in Albino Rats after Aluminum Chloride Exposure and Possible Protective Role of Omega 3

Sulayman Alhasy ZMA[1], Maher IA[2], Morsy MM[2] and Shehata MA[2*]

[1]Department of Anatomy and Embryology, Faculty of Medicine, Omar Almoktar University, Libya
[2]Department of Anatomy and Embryology, Faculty of Medicine, Zagazig University, Egypt

Abstract

Background: During the last decades, human exposure to Aluminum (AL) is markedly increased as it presents in drinking water, manufactured food and in several medicines like buffered aspirin and antacids. Omega-3 possesses a wide range of beneficial effects and plays a role in the treatment of different forms of chronic lung diseases.

Aim of the study: To evaluate the possible effect of Aluminum chloride in the structure of the lung in postnatal albino rats and the possible protective role of Omega 3 using a light microscope, immunohistochemistry, and morphometric study.

Materials and Methods: 48 female rats of Wistar strain were divided into 4 groups. Treatment was carried out by the 14th day of pregnancy until day 14 after delivery. Pups of all groups were sacrificed at 14th and 21st days postnatal. Group I was given water and a balanced diet by gastric intubation. Group II each rat gavaged orally with Omega 3 (20 mg/kg b.w) dissolved in corn oil once daily. Group III each rat was given orally aluminum chloride (475 mg/l equivalent to 76 mg/kg BW, orally) dissolved in water. Group IV rats gavage orally with Omega 3 (20 mg/kg) and aluminum chloride (475 mg/l equivalent 76 mg/kg BW, orally).

Results: On day 14 there is severe destruction of the bronchial mucosal lining and the nearby bronchial vessel. Besides, highly congested bronchial vessels (CBV), as well as, prominent thick interalveolar septa and variably sized sacculations are seen. At day 21st postnatal: H & E stained sections of lung showing congested bronchial vessel and small bronchioles with intra-bronchiolar hemorrhage and exudate. Omega 3 protected group shows an improvement of the previous results.

Conclusion: Aluminum chloride affects the normal development of the lung. The use of Omega 3 compounds reduces the toxic effects caused by aluminum chloride exposure.

Keywords: Aluminum chloride; Omega 3, Lung; Albino rats

Correspondence to: Mohammed Ahmed Shehata, Department of Anatomy and Embryology, Faculty of Medicine, Zagazig University, Egypt; E-mail: dr.mohammed.shehata2007@gmail.com

Citation: Sulayman Alhasy ZMA, Maher IA, Morsy MM, Shehata MM (2020) Postnatal Changes of Lung Structure in Albino Rats after Aluminum Chloride Exposure and Possible Protective Role of Omega 3. Prensa Med Argent, Volume 106:4. 225. DOI: https://doi.org/10.47275/0032-745X-225.

Received: February 27, 2020; **Accepted:** March 23, 2020; **Published:** March 26, 2020

Introduction

Aluminium is 8% of metallic element in addition, the third most common metal. Naturally it presents in environment as silicate, oxides and hydroxides as well as combined with elements as sodium and fluoride, the aluminium is flexible metal and silver-white in colour, in our bodies it is poorly absorbed and well eliminated, if absorption occurs the distribution mainly in brain, kidney, bone, testes, and liver [1]. In the industry, the aluminium powders are used in paints and pigments, and insert in fuel industry. The Aluminium oxides are used as food and the production of refractories, ceramics, electrical insulators, glass and heat resistant fibres. In medical part, the Aluminium is used in pharmaceutical and personal care product. [2]. Aluminium is added to drinking water in water purification as aluminium sulphate. In pharmaceutical industry many medications containing aluminium as topical solutions or as drugs such as aspirin, analgesic, antipyretic, and antacids. Aluminium is also found in infant formulae human and cow milk [3]. Baxter R, et al. (2008) mentioned that aluminium hydroxide is prescribed as medication to lower plasma phosphorus levels in kidney failure patients [1]. In addition, dentists use aluminium silicate as component of dental cement. Lastly the aluminium chloride enters rubber industry as lubricants, food preservatives, and cosmetics. Omega-3 are polyunsaturated fatty acids and are divided into 2 classes, Omega 3 (n-3) and Omega6 (n-6). Therefore, PUFAs is called essential fatty acids that act as energy substrates and integral membrane components. They play vital role in the preservation of nervous system [4]. In addition to ant inflammation, proresolving lipid mediators, reduction of triglycerides, antithrombotic and ant arrhythmic effects. In addition to fatty acid synthesis gene expression and up-regulate gene expression in FA oxidation [5]. The lungs represent the major part of

respiratory system. It consists mainly of spongy tissue and conducting air tubules called bronchi and bronchioles. The spongy tissue takes place between air and blood are forming alveolar duct and alveoli [6]. The lung development has been divided into: saccular stage, embryonic stage, canalicular stage, pseudo glandular stage, and alveolar stage. The alveolar stage is split in two and a 6th stage was defined as the stage of micro vascular maturation. These stages are a specific developmental milestone [7-9]. Many studies have proved that Aluminum has toxic effects on several organs. Buraimoh AA, et al. (2013) suggested that Aluminum Chloride has effects on the lung histology of Wister rats, which were eminent in the form of hemorrhage and congested blood vessels [10].

Material and Methods

Materials

Chemicals: The chemical substances used are (1) Aluminum chloride anhydrous extra pure (Al Cl3) was obtained from Research-Lab Fine Chemicals Industries, India, through El-Goumhouria Company Medicines, in the form of silvery white crystals with a molecular weight of 133.34. Aluminum chloride powder was dissolved using water. A dose of aluminum chloride was 475 mg/kg B.W. [10]. Each rat received 1 ml distilled water containing 76 mg aluminum chloride orally. (2) Omega 3 was taken as soft gels tablet contain 1000 mg yellow in color made in USA the dose of Omega 3 is 20 mg per kg dissolved in corn oil orally. (3) Corn oil to dissolve 0mega 3 obtained from market.

Animals: 48 virgin female albino rats and 24 male albino rats of 160-200 gm were obtained from Zagazig University. Temperature was kept at 25~30℃. A cycle of twelve hours of Light and twelve hours of darkness was maintained throughout this study. All animals received food and tap water ad libtium.

Determination of pregnancy

Animals were mated overnight, after that separated, and examined in the following morning for sperm. Vaginal smears stained with Papanicolaou stain were taken every day. When smear was positive, the first day of pregnancy was considered. The females with negative vaginal smear were also isolated and re kept again with males. The process was repeated until all females became pregnant.

Classification of groups

The length of gestation for animals averaged 22 days. 48 pregnant female rats were divided to 4 groups of twelve each. Pups were sacrificed at 14th and 21st days postnatal.

Group I (negative control group): This group contained 12 pregnant rats which were not received any treatment and were given water and balanced diet by gastric intubation. The offspring of these pregnant rats are subdivided into 2 subgroups

- Subgroup Ia14PND: contains 6 mothers with their pups.
- Subgroup Ib21PND; contains 6 mothers with their pups

Group II (Positive control group): Each rat gavaged orally with Omega 3 (20 mg/kg b.w) dissolved in corn oil once daily [11]. The offspring of these pregnant rats are subdivided into 2 subgroups

- Subgroup IIa14PND: contains 6 mothers with their pups.
- Subgroup IIb21PND; contains 6 mothers with their pups

Group III (Aluminum chloride-treated group): Each rat was given orally aluminum chloride (475 mg/l (76 mg/kg BW), orally) dissolved in distilled water [12]. The offspring of these pregnant rats are subdivided into 2 subgroups

- Subgroup IIIa14PND: contains 6 mothers with their pups.
- Subgroup IIIb21PND; contains 6 mothers with their pups

Group IV (Aluminum chloride and Omega 3 group): Rat's gavage orally with Omega 3 (20 mg/kg) and aluminum chloride (475 mg/l equivalent to 76 mg/kg BW, orally). The offspring of these pregnant rats are subdivided into 2 subgroups

- Subgroup IVa14PND: contains 6 mothers with their pups.
- Subgroup IVb21PND; contain 6 mothers with their pups.

Pups were taken and separated to be sacrificed on day 14 and 21 after parturition. Pups were anesthetized to avoid stress. Histopathological examination of lung tissue was done. Samples are rinsed and homogenized (10%) in Tris-HCl.

Histopathological Examination

Samples fixed in Bouin's solution, then dehydrated in alcohols, cleared in xylene and embedded in paraffin. The slides stained by hematoxylin and Eosin and Masson's Trichrome [13].

Immunohistochemical Study

Immunohistochemical reactions were carried out on sections of the lung using an antibody against ASMA marker to muscle specific protein around epithelial tube [14]. A mouse anti alpha muscle (1A4, Sigma, USA) diluted as supplied (1:800) and designed for the specific localization of ASMA in paraffin sections. They were delivered from DAKO life trade Egypt. A biotinylated secondary anti-immunoglobulin capable of binding and streptavidinbiotin enzyme complex since both primary antibody and antibody of the label are produced in the same animal species. Sections were mounted on positively charged glass slides. The slides were incubated at 37℃ overnight for accurate adhesion of the sections to the slides. Slides placed in 60 C of 13 to 18 h. It was transferred into three changes of fresh xylene for 10 minutes each change. Slides were transferred into graded ethanol (two changes of 100%, two changes of 95%, two changes of 70% and two changes of 50%), 3 min for each change. The pH (7.2) of the buffer was checked with each run. The primary antibody replaced by buffer was included for each specimen, stained with Mayer's hematoxylin and was first noted to determine the amount of specific staining seen in the examined sections.

Morphometric Study

Non- overlapping five images were randomly taken from each section. At least three randomly selected sections were analyzed per animal (3 animals from each group) on a light microscope using a colored camera. The total area and the terminal segment area were then measured in pixels using (Image analyzer, LEICA DN500). The measurements are performed on H, E, and Masson Trichrome sections. The mean values for each parameter in different groups were determined.

Statistical Analysis

The data obtained from the image analyzer were analyzed by student's t test using analysis program SPSS V.15. with a p value less than 0.05 (the level of significance). The following statistical methods were used for analysis of results of the present study [15]:

• Image analysis and morphometry was performed by ImageJ (FIJI) software. For the sections stained by Hematoxylin and eosin. The area percentage of collagen was assessed in sections stained by Masson's Trichrome. As well as, the area percentage of α-SMA expression was assessed in sections treated with α-SMA.

• The collected data were computerized and statistically analyzed using Graph Pad Prism 5.01. Quantitative data were expressed as (Standard deviation).

• Differences between mean values of experimental groups are tested with ANOVA. Turkey's multiple test was carried out as post hoc test of ANOVA.

Results

These Examinations are conducted for the groups.

Group I (Negative control group)-Light microscopic examination

Subgroup Ia: Age 14th postnatal

Hematoxylin and Eosin (H&E): Examination of H&E stained sections from rat lung at 14th post-natal day revealed that the rat lung was formed of air saccules divided by large numbers of developing crests (secondary septa) which recognized along the primary septa into smaller units (primitive alveoli) (Figure 1). The wall of bronchioles consists of ciliated cuboidal epithelium (Figure 2). Primitive alveoli were lined by flattened I pneumocytes and cuboidal II pneumocytes (Figure 3).

Masson's trichrome stain: Masson's trichrome stained sections showed ordinary amount of collagen fibers in the wall of the bronchioles and bronchial vessels. In addition, the surrounding lung tissue demonstrates minimal amount of collagen fibers in the interalveolar septa (Figure 4).

α SMA Immunostaining: Immunoperoxidase technique for SMA

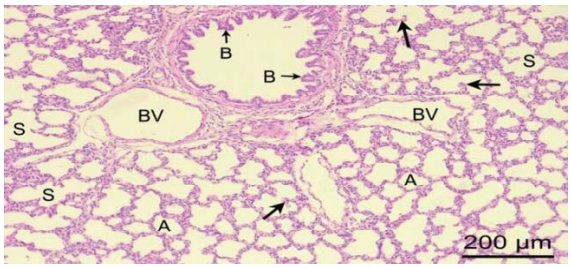

Figure 1: A photomicrograph of a section in the lung of the control group at 14 DPN showing medium sized bronchiolar wall (B) with the lining respiratory epithelium and bronchial vessels (BV), primitive alveoli (A), air saccules (S), and secondary septa (arrow). (H&E x 100).

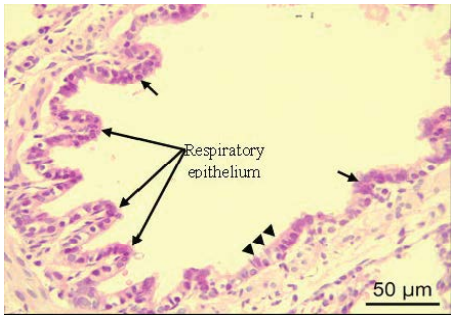

Figure 2: A photomicrograph of previous section with magnified medium sized bronchiolar wall showing wall of bronchioles which consists of respiratory epithelium, ciliated cells (arrow) and Clara cells (arrow heads) (H&E X 400).

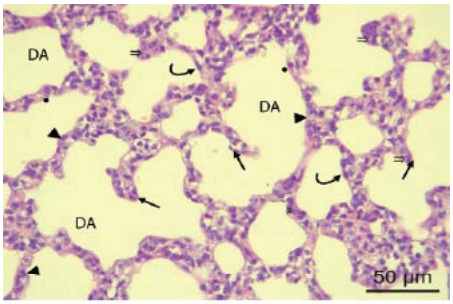

Figure 3: A photomicrograph of previous section with magnified surrounding lung tissue showing developing alveoli (DA), secondary septa(arrow), primary septa (*), capillary network (double arrow), flattened type I pneumocytes (curved arrow) and cuboidal type II pneumocytes (arrow heads) (H&E × 400).

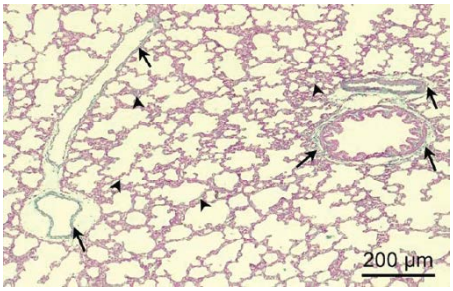

Figure 4: A photomicrograph in the lung of the control group at 14 DPN showing ordinary amounts of collagen fibers (Green) in the wall of the bronchioles and bronchial vessels (arrows). In addition, the surrounding lung tissue demonstrates minimal amount of collagen fibers (Green) in the interalveolar septa (arrow heads). (Masson's trichrome X 100)

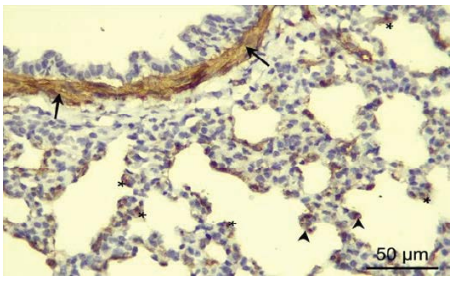

Figure 5: A photomicrograph of a section in the lung of control group at 14 DPN showing prominent expression of α-SMA in the wall of the bronchi (arrows). In addition, α SMA - ® positive cells in the primitive alveolar septa (*) and other α SMA - ® positive cells in the developing secondary septa (arrow heads) are clearly demonstrated (α SMA × 400).

showed a population of round α SMA –® positive cells appeared at the tips of the developing secondary septa in addition to the slender α SMA-® positive cells in primitive septa (Figure 5).

Subgroup Ib: Age 21th day postnatal

Hematoxylin and Eosin (H&E): Examination of H & E stained sections of lung at 21st postnatal day revealed normal architecture of alveoli with many alveolar sacs. Alveoli were separated by apparently thin primary septa (Figure 6). Alveoli were lined by squamous pneumocytes type I cell and cuboidal pneumocytes type II cell. Alveolar walls were less cellular with thin interstitium but groups of interstitial cells were observed where several septa were joined. The double capillary layers inside the primary and secondary septa are transformed into a single central capillary layer (Figure 7). The terminal bronchiole is lined by simple columnar epithelium and surrounded by thin layer of smooth muscle (Figure 8).

Masson's trichrome stain: Masson's trichrome stained sections of 21st DPN showing average amount of collagen fibers in the wall of the bronchi and bronchial vessels. In addition, the surrounding lung tissue

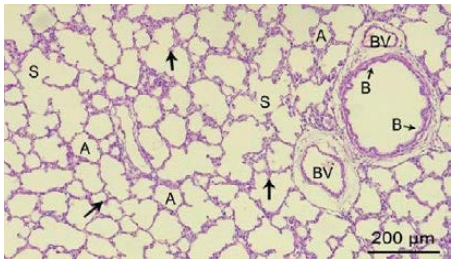

Figure 6: A photomicrograph of a section in the lung of the control group at 21 DPN showing medium sized bronchiolar wall (B) with the lining respiratory epithelium and bronchial vessels (BV). In addition, air saccules (S), secondary septa (arrow) and primitive alveoli (A) with thin interalveolar septa are also seen (H&E X 100)

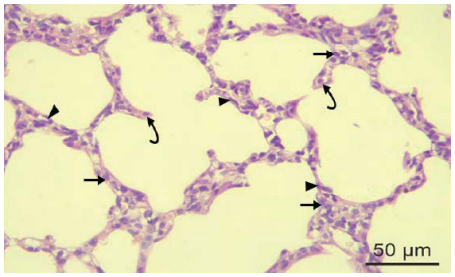

Figure 7: A photomicrograph with magnified surrounding lung tissue showing Alveoli lined by squamous pneumocytes I cell (arrow heads), and cuboidal pneumocytes II cell (arrows). Secondary septa with single central capillary layer (curved arrow) (×400).

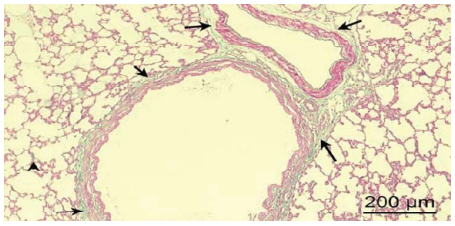

Figure 8: A photomicrograph of the control group at 21 DPN showing average amounts of collagen fibers (Green) in bronchial vessels (arrows). In addition, the surrounding lung tissue demonstrates scarce amount of collagen fibers (Green) in the interalveolar septa (arrow heads). (Masson's trichrome X 100).

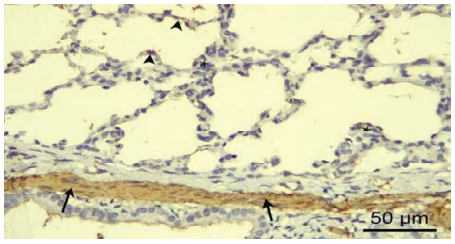

Figure 9: A photomicrograph in the lung of the control group at 21 DPN prominent expression of α-SMA in the wall of the bronchi (arrows). In addition, α-SMA–positive cells in the interstitial tissue of immature alveoli (*) and other α-SMA–positive cells in the developing secondary septa (arrow heads) are visible (α-SMA X 400).

demonstrates scattered amount of collagen fibers in the interalveolar septa (Figure 8).

α SMA Immunostaining: Immunoperoxidase technique for α SMA showed a round α SMA - ® positive cells at the tips of the developing secondary septa, whereas the slender α SMA - ® positive interstitial cells in the primary septa are disappeared (Figure 9).

Group II

Subgroup IIa: Age 14th postnatal

Hematoxylin and Eosin (H&E): Sections of lung at 14th postnatal

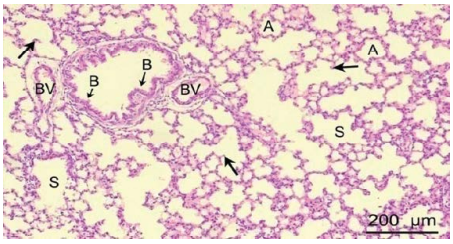

Figure 10: A photomicrograph of a section in the lung of the group treated with Omega3 at 14 DPN showing medium sized bronchiolar wall (B) with the lining respiratory epithelium and bronchial vessels (BV). In addition, air saccules (S), secondary septa (arrow) and primitive alveoli (A) are visible (H&E X 100).

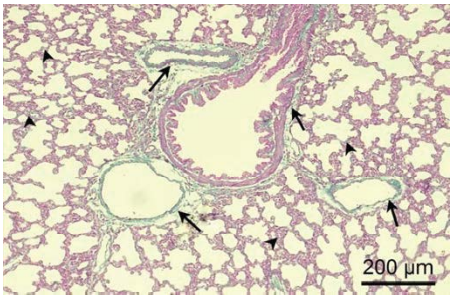

Figure 11: A photomicrograph in the lung of group supplemented with Omega3 at 14 DPN showing the common amount of collagen fiber (Green) in the bronchioles and bronchial vessels (arrows). In addition, the surrounding lung tissue demonstrates minimal amount of collagen fibers (Green). (Masson's trichrome X 100).

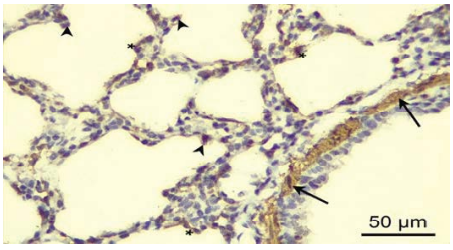

Figure 12: A photomicrograph of a section in the lung of Omega3 group at 14 DPN showing average expression of α-SMA in the wall of the bronchi (arrows). In addition, α-SMA–® positive cells in the primitive alveolar septa (*) and other α-SMA–® positive cells in the developing secondary septa (arrow heads) are clearly demonstrated (α-SMA X 400).

day group treated with Omega 3 was formed mainly of medium sized bronchiole with the lining respiratory epithelium and bronchial vessels, air saccules, secondary septa and primitive alveoli (Figure 10).

Masson's Trichrome stain: Masson's trichrome stained sections showed ordinary amount of collagen fibers in the wall of the bronchioles and bronchial vessels. In addition, the surrounding lung tissue demonstrates minimal amount of collagen fibers in the interalveolar septa (Figure 11).

α SMA Immunostaining: Immunohistochemical stained sections showing prominent expression of α-SMA in the wall of the bronchi. In addition, α-SMA–positive cells in the primitive alveolar septa are demonstrated (Figure 12).

Subgroup II b: Age 21th postnatal

Hematoxylin and Eosin (H&E): The respiratory portion of the lung was formed mainly of medium sized bronchiole with healthy lining respiratory epithelium and bronchial vessels, air saccules with thin interalveolar septa, secondary septa and primitive alveoli (Figure 13).

Masson's Trichrome stain: Masson's trichrome stained sections showing ordinary amount of collagen fibers in the wall of the bronchi

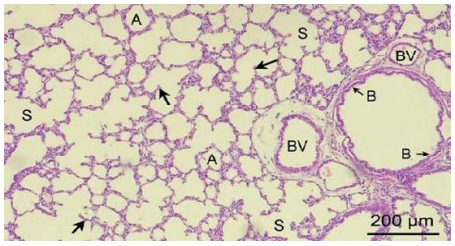

Figure 13: A photomicrograph of a section in the lung of the Omega3 group at 21 DPN showing medium sized bronchiolar wall (B) with healthy lining respiratory epithelium and bronchial vessels (BV). In addition, air saccules with thin interalveolar septa (S), secondary septa (arrow) and primitive alveoli (A) are seen (H&E X 100).

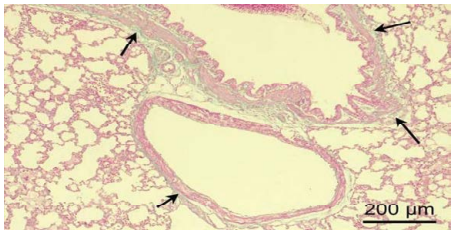

Figure 14: A photomicrograph of group supplemented with Omega3 at 21 DPN showing ordinary amount of collagen fiber (Green) in the bronchi and bronchial vessels (arrows). In addition, the surrounding lung tissue demonstrates non-visible collagen fibers in the interalveolar septa. (Masson's trichrome X 100).

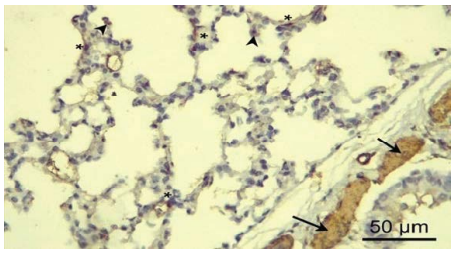

Figure 15: A photomicrograph of Omega3 group at 21 DPN showing average expression of α-SMA in the wall of the bronchi (arrows). In addition, α-SMA–positive cells in the interstitial tissue of immature alveoli (*) and other α-SMA–positive cells in the developing secondary septa (arrow heads) are clearly demonstrated (α-SMA X 400).

and bronchial vessels. In addition, the surrounding lung tissue demonstrates non-visible collagen fiber (Figure 14).

α SMA Immunostaining: Immunohistochemical stained sections showing average expression of α-SMA in the wall of the bronchi. In addition, α-SMA–positive cells in the interstitial tissue of immature alveoli and other α-SMA–positive cells in the developing secondary septa are demonstrated (Figure 15).

Group III (Aluminum chloride-treated group)

Subgroup III a: Age 14th postnatal

Hematoxylin and eosin (H&E): Examination of H & E stained sections of lung at 14th postnatal day showing bronchiole with sever destruction of the mucosal lining and the nearby bronchial vessel. In addition, para-bronchial inflammatory infiltration and multiple sacculations are seen in the lung tissue. Also dark stained nuclei and vacuolated cells are seen (Figure 16). Other section showing large highly congested bronchial vessel (CBV). As well as, the surrounding lung tissue showing prominent thick interalveolar septa and variably sized sacculations (Figure 17). Also bronchial vessels (BV), with sever congested, thickened walls are seen. In addition, the alveoli demonstrated high degree of sacculations, interstitial infiltration, exudation and consolidation

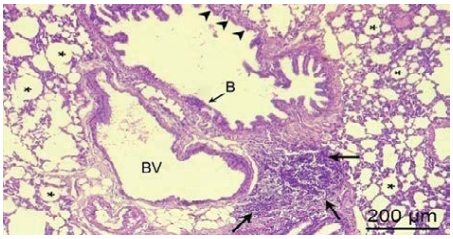

Figure 16: A photomicrograph of the group treated with Al Cl3 at 14 DPN showing large bronchiolar wall (B) with sever destruction of the mucosal lining (arrow heads) and the nearby bronchial vessel (BV). In addition, para-bronchial inflammatory infiltration (arrows) and multiple sacculations in the lung tissue (*) are seen (H&E X 100).

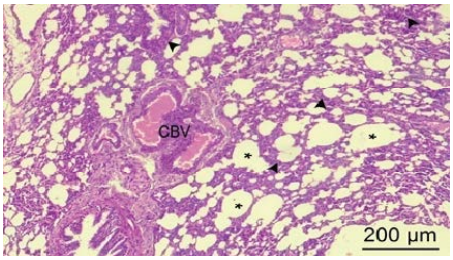

Figure 17: A photomicrograph of a section in the lung of the group treated with Al Cl3 at 14 DPN showing large highly congested bronchial vessel (CBV). As well as, the surrounding lung tissue shows prominent thick interalveolar septa (arrow head) and variably sized sacculations (*) (H&E X 100).

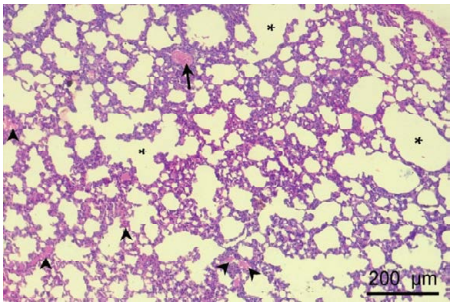

Figure 18: A photomicrograph of group treated with Al Cl3 at 14 DPN showing congested bronchial vessel (arrow), intra-alveolar extravasations and exudate (arrow heads). In addition, the alveoli demonstrated high degree of sacculations (*) (H&E X 100).

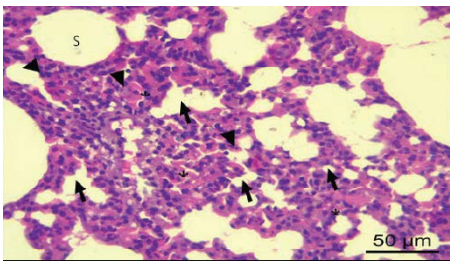

Figure 19: A photomicrograph of group treated with Al Cl3 at 14 DPN showing surrounding lung tissue with saccules(S), collapsed alveoli(arrows), dark stained nuclei (arrow heads), intra-bronchiolar hemorrhage and exudate (*) (H&E X 400).

(Figure 18). Also saccules (S), collapsed alveoli with dark stained nuclei, intra-bronchiolar hemorrhage and exudate are observed. (Figure 19).

Masson's Trichrome stain: Masson's trichrome stained sections showing very high content of collagen fibers in the wall of bronchioles and bronchial vessels. In addition, the surrounding lung tissue demonstrates abundant collagen fibers in the inter-alveolar septa (Figure 20).

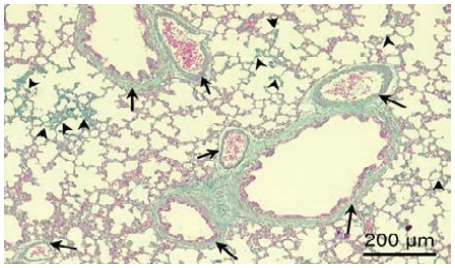

Figure 20: A photomicrograph of a section in the lung of Al Cl3 treated group at 14 DPN showing very high content of collagen fibers (Green) in the wall of bronchioles and bronchial vessels (arrows). In addition, the surrounding lung tissue demonstrates abundant collagen fibers (Green) in the inter-alveolar septa (arrow heads) (Masson's trichrome X 100).

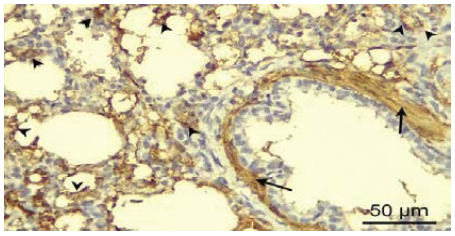

Figure 21: A photomicrograph of a section in the lung of Al Cl3 treated group at 14 DPN showing abundant expression of α-SMA in the wall of the bronchi (arrows). As well as, multiple alveoli with thick interalveolar septa and sacculations displaying highly prominent expression of α-SMA in several areas of the alveolar tissue (arrow heads) (α-SMA X 400).

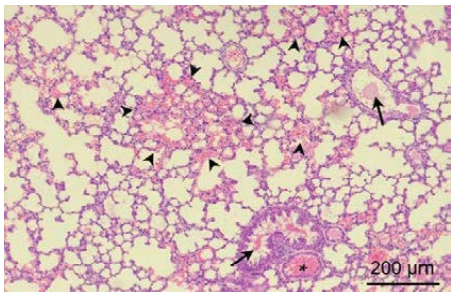

Figure 22: A photomicrograph of the group treated with Al Cl3 at 21 DPN showing congested bronchial vessel (*) and small bronchioles with intra-bronchiolar hemorrhage and exudate (arrows). The surrounding lung tissue displays multiple foci of massive intra-alveolar hemorrhage (arrow heads) (H&E X 100).

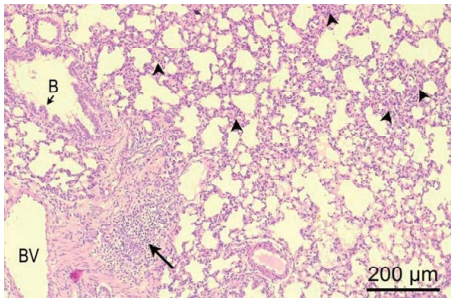

Figure 23: A photomicrograph of group treated with Al Cl3 at 21 DPN showing medium sized bronchiole (B) with destruction of epithelial lining and the nearby bronchial vessel (BV). In-between inflammatory infiltration focus (arrow) and multiple foci of interstitial infiltration (arrow heads) are prominent (H&E X 100).

α SMA Immunostaining: Immunohistochemical stained sections showing abundant expression of α-SMA in the wall of the bronchi. As well as, multiple alveoli with thick interalveolar septa and sacculations displaying highly prominent expression of α-SMA are noticed in several areas of the alveolar tissue (Figure 21).

Subgroup IIIb: Age 21th postnatal

Hematoxylin and Eosin (H&E): Examination of H & E stained sections of lung showing congested bronchial vessel and small bronchioles with intra-bronchiolar hemorrhage and exudate. The surrounding lung tissue displays multiple foci of massive intra-alveolar hemorrhage, interstitial hemorrhage and exudate (Figure 22). Other section-showing medium sized bronchiole and the nearby bronchial vessel. In-between inflammatory infiltration focus and multiple foci of interstitial infiltration are prominent (Figure 23). Sever destruction of epithelial lining (arrow heads) is seen. Other sections showing multiple foci of peri-bronchiolar inflammatory infiltration destroying the wall of the bronchiole, discrete foci of interstitial infiltration and consolidation, some air sacculations and prominent thick inter-alveolar septa are found (Figure 24).

Masson's Trichrome stain: Masson's trichrome stained sections showing higher content of collagen fiber in wall of bronchioles, bronchial vessels and peri-bronchial infiltration. In addition, the

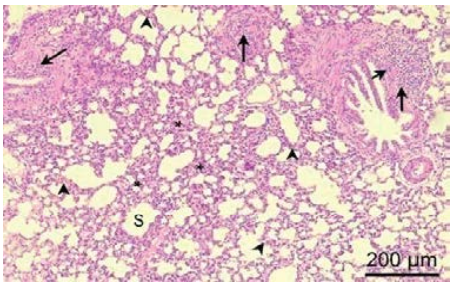

Figure 24: A photomicrograph of group treated with Al Cl3 at 21 DPN showing multiple foci of peri-bronchiolar inflammatory infiltration (arrow) destroying the wall of the bronchiole, discrete foci of interstitial infiltration and consolidation (*), some air sacculations (S) and prominent thick inter-alveolar septa (arrow head) are seen (H&E X 100).

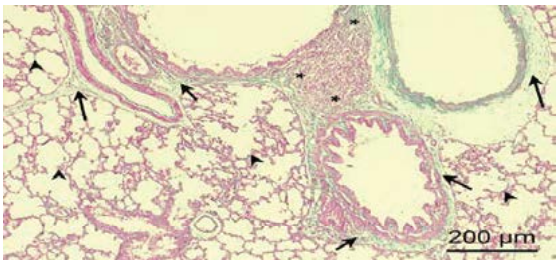

Figure 25: A Photomicrograph of Al Cl3 treated group at 21 DPN showing higher content of collagen fiber (Green) of bronchioles, bronchial vessels (arrows) and peri-bronchial infiltration (*). In addition, the surrounding lung tissue demonstrates abundant collagen fibers (Green) in the inter-alveolar septa (arrow heads). (Masson's trichrome X 100).

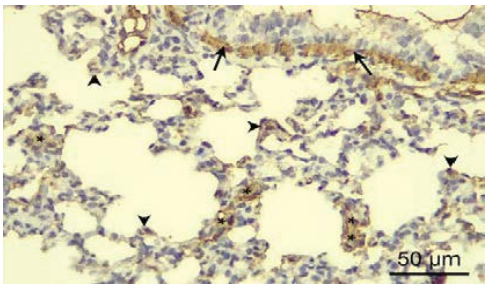

Figure 26: A Photomicrograph of Al Cl3 treated group at 21 DPN showing abundant expression of α-SMA in the wall of the bronchi (arrows). As well as, multiple alveoli with thick interalveolar septa and sacculations displaying highly prominent expression of α-SMA in the primitive septa (arrow heads) and interstitial tissue (*) (α-SMA X 400).

surrounding lung tissue demonstrates abundant collagen fibers in the inter-alveolar septa (Figure 25).

α SMA Immunostaining: Immunohistochemical stained sections showing abundant expression of α-SMA in the wall of the bronchi. As well as, multiple alveoli with thick interalveolar septa and sacculations displaying highly prominent expression of α-SMA in the primitive septa and interstitial tissue (Figure 26).

Group IV (Aluminum chloride and Omega 3 group)

Subgroup IVa: Age 14th postnatal

Hematoxylin and eosin (H&E): Examination showing multiple small bronchioles and bronchial vessel surrounded by abundant lung tissue with air saccules and primitive alveoli. However, multiple foci with interstitial infiltration, extravasations and exudation are still seen. In addition, destruction of epithelial lining is still present and alveolar surrounding is improved. (Figure 27).

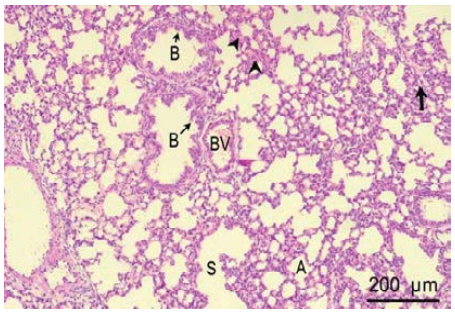

Figure 27: A photomicrograph of the group treated with Al Cl3+Omega3 at 14 DPN showing multiple small bronchiolar walls (B) and bronchial vessel (BV) surrounded by abundant lung tissue showing, air saccules (S) and primitive alveoli (A). However, multiple foci with interstitial infiltration (arrow), extravasations and exudation (arrow heads) are prominent (H&E X 100).

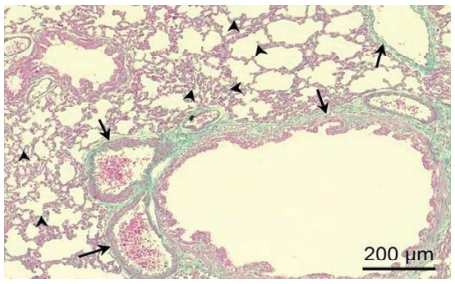

Figure 28: A photomicrograph of the group received Al Cl3+Omega3 at 14 DPN showing average amount of collagen fiber (Green) in bronchi and bronchial vessels (arrows). However, the surrounding lung tissue displayed abundant amount of collagen fibers more than average (Green) in the interalveolar septa (arrow heads) (Masson's trichrome X 100).

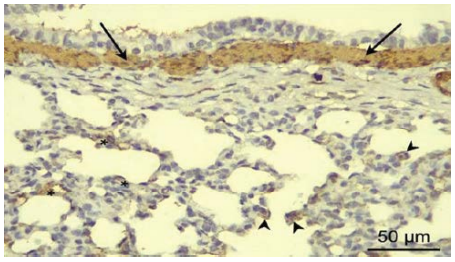

Figure 29: A photomicrograph of a section in the lung of Al Cl3+Omega3 group at 14 DPN showing ordinary expression of α-SMA in the wall of the bronchi (arrows). As well as, α-SMA–positive cells in the primitive alveolar septa (*) and in the developing secondary septa (arrow heads) are prominent (α-SMA X 400).

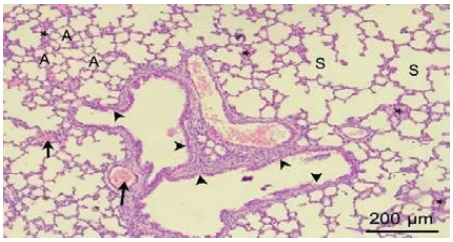

Figure 30: A Photomicrograph of the group received Al Cl3+Omega3 at 21 DPN showing 2 bronchioles with sloughed respiratory mucosa (arrow heads), congested small bronchial and parenchymal vessels (arrow). In addition, multiple air saccules (S) and primitive alveoli (A) with average septal thickness are present. However, foci of intra-alveolar infiltration (*) are discrete (H&E X 100).

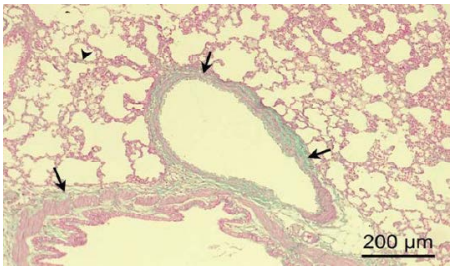

Figure 31: A photomicrograph of the group received Al Cl3+Omega3 at 21 DPN showing the common amount of collagen fiber (Green) in bronchi and bronchial vessels (arrows). As well as, the surrounding lung tissue displayed average amount of collagen fibers (Green) in the interalveolar septa (arrow heads) (Masson's trichrome X 100).

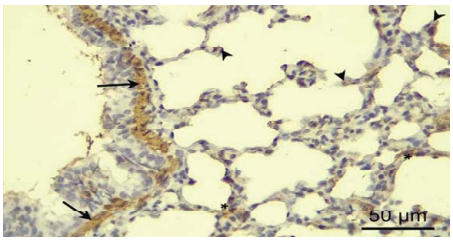

Figure 32: A photomicrograph of a section in the lung of Al Cl3+Omega3 group at 21 DPN showing ordinary expression of α-SMA in the wall of the bronchi (arrows). As well as, α-SMA–positive cells in the tips of secondary septa (arrow heads) and in the interstitial tissue of immature alveoli (*) (α-SMA X 400).

Masson's Trichrome stain: Masson's trichrome stained sections showing average amount of collagen fibers in the wall of the bronchi and bronchial vessels. However, the surrounding lung tissue displayed abundant amount of collagen fiber more than average (Figure 28)

α SMA Immunostaining: Immunohistochemical stained sections showing ordinary expression of α-SMA in the wall of the bronchi. As well as, α-SMA–positive cells in the primitive alveolar septa and in the developing secondary septa are prominent (Figure 29).

Subgroup IVb: Age 21th postnatal

Hematoxylin and eosin (H&E): Examination of H & E stained sections showing 2 bronchioles with sloughed respiratory mucosa, congested small bronchial and parenchymal vessels. In addition, multiple air saccules and primitive alveoli with average septal thickness. However, foci of intra-alveolar infiltration are discrete. (Figure 30).

Masson's Trichrome stain: Masson's trichrome stained sections showing the common amount of collagen fibers in the wall of the bronchi and bronchial vessels. As well as, the surrounding lung tissue displayed average amount of collagen fibers. (Figure 31).

α SMA Immunostaining: Immunohistochemical stained sections

Table 1: Statistical comparison between mean values of different morphometric parameters in different studied groups at the age 14 PND.

Parameter	Control Means ± SD	Omega3 Means ± SD	Al Cl3 Means ± SD	Al Cl3+Omega3 Means ± SD	ANOVA
Thickness of inter-alveolar septa (µm)	5.48 ± 1.272	5.46 ± 0.651 Ns	9.54 ± 0.867***	7.29 ± 1.147***	<0.0001***
ATETAS (%)	38.24 ± 2.875	38.57 ± 2.813 Ns	44.04 ± 3.608**	39.71 ± 2.398*	0.0017***
Area percentage of collagen (%)	5.80 ± 1.314	6.30 ± 0.590 Ns	12.46 ± 1.824***	10.18 ± 0.855**	<0.0001***
Area percentage of α-SMA (%)	4.07 ± 0.422	4.16 ± 0.443 Ns	7.51 ± 0.396***	6.48 ± 0.899**	<0.0001***

Where: SD = Standard Deviation; *(highly significant); *(moderately significant); *(mildly significant); Ns: Not significant; and *p = Significant.

Table 2: (21 PND) Morphometry table: Statistical comparison between mean values of different morphometric parameters in different studied groups at the age 21PND.

Parameter	Control Means ± SD	Omega3 Means ± SD	AlCl3 Means ± SD	AlCl3+Omega3 Means ± SD	ANOVA
Thickness of inter-alveolar septa (µm)	3.55 ± 0.512	3.55 ± 0.536 Ns	4.96 ± 0.760***	3.91 ± 0.582**	0.0001***
ATETAS (%)	31.00 ± 2.275	29.73 ± 3.326 Ns	44.70 ± 2.719***	40.02 ± 2.686*	<0.0001***
Area percentage of collagen (%)	5.58 ± 1.429	5.73 ± 1.237 Ns	16.62 ± 3.924***	9.55 ± 1.231***	<0.0001 7***
Area percentage of α-SMA (%)	2.90 ± 0.427	2.79 ± 0.574 Ns	4.51 ± 0.302***	3.65 ± 0.351**	<0.0001***

showing ordinary expression of α-SMA in the wall of the bronchi. As well as, α-SMA–positive cells in the interstitial tissue of immature alveoli. (Figure 32).

Morphometrical Results

Omega 3 and Al Cl_3 groups were compared to the control group. However, Al Cl3+Omega 3 group was compared to Al Cl3 group (Table 1).

The results were statistically significant when P <0.05. Different stages of significance were considered. High significance (***) when P value < 0.001, Moderate significant (**) at 0.01 >P value >0.001 and low significance (*) when 0.05 >P value >0.01 (Table 2).

Discussion

The AL is the 3rd metal in the earth [16]. That naturally presents in water (e.g. ponds, lakes and streams). So that, human is exposed to a little amount of AL from drinking water [17]. The current study was make to detect Aluminum chloride effect, beside its mechanism of action and the possible protective role of Omega 3. The rat was chosen as it is considered to be the first animal to be domesticated for strictly scientific purposes and become a species of choice because of metabolic similarities, as well as their small size and short life span. In the current study embryos were exposed to Aluminum chloride from the 14th day of pregnancy until day14 after delivery. This age corresponds to lung development which has been divided into 5 stages. The present work revealed diffuse affection of the lung tissue and loss of the normal alveolar architecture in response to aluminum administration. Riihimäki and Aitio (2012) declared that lung epithelium may be a site for the accumulation of aluminum and a surface for its uptake into lung tissues and access to the systemic circulation [6].

In the current study, the control group at age 14th day postnatal shows air saccules and secondary septa that appear as finger like projection which divided air space to primitive alveoli this was similar to what. Bolle I, et al. (2007) and Joshi and Kotecha (2007) said [8,18].

In addition there were several characteristic features shown in the lung at this age group as respiratory epithelium, ciliated cells and Clara cells. This description was in accordance with Ross MH, et al. (2009) [19]. Also, the surrounding lung tissue show developing alveoli, secondary septa, primary septa, capillary network, flattened I pneumocytes and cuboidal II pneumocytes. This description was in accordance with Tomashefski JF, et al. (2008) [20]. These septa contain double capillary layer. This was in agreement with Prodhan P, et al. (2002), Roth-Kleiner M, et al. (2005) and Joshi & Kotecha (2007), who stated that the formation of the pulmonary alveoli as shown in the present study was initiated by developing of secondary septa from the pre- existed primary septa [21,22,8]. These secondary septa subdivided. All the primary and secondary septa explained a double capillary network. The interalveolar walls contain only a capillary layer.

Masson's trichrome stained sections show amount of collagen fibers in the wall of the bronchioles and bronchial vessels, the surrounding lung tissue demonstrates minimal amount of collagen fibers. This description was in accordance with Ahmed RR, et al. (2009) who found that minimal amount of collagen fibers was concentrated mainly around bronchus and blood vessels [23]. α-SMA immunohistochemical stained sections showed prominent expression of α-SMA in the wall of the bronchi as well as, α-SMA–positive cells and other α-SMA-positive cells in the developing secondary septa are clearly demonstrated. This description was in accordance with Ibáñez-Vea M, et al. (2018) who demonstrated the lung compartment specific expression of α-SMA positive cells, which are apparently myofibroblasts, in alveoli, bronchioles and bronchi in lung tissue [24]. Lastly α-SMA is a useful marker for smooth muscle because of its consistent appearance in bronchiolar smooth muscle. By the use of this marker, we could succeed in clarifying the early differentiation and later distribution of vascular smooth muscle cells (Mitchell et al., 1990). In the current study, the control group at age 21st day postnatal shows bronchiolar wall with the lining respiratory epithelium and bronchial vessels, air saccules, secondary septa and primitive alveoli with thin interalveolar septa. This description was in accordance with Ross and Pawlina (2009) who said that the surrounding lung tissue show alveoli lined by squamous pneumocytes I cell, cuboidal pneumocytes II cell and secondary septa with single central capillary layer. The double capillary layers inside the primary and secondary septa are transformed to a single capillary layer, this agreed with Schittny JC and Burri PH (2007) who stated that the essence of this stage is the restructuring of the double capillary networks in the parenchymal septa to the mature aspect with a single capillary system [9]. Masson's trichrome stained sections show average amount of collagen fibers. In addition, the surrounding lung tissue demonstrates scarce amount of collagen fibers. This description was in accordance with Prokopakis E, et al. (2013) who noticed the presence of minimal amount of collagen in alveolar wall, bronchi, bronchial vessels, the interstitial tissue of immature alveoli and the developing secondary

septa [25]. This description was in accordance with Warburton D, et al. (2005) who stated that the round α-SMA-positive cells persist in the tips of the secondary septa whereas the slender α-SMA-positive in the primary septa disappeared in mature alveoli but persisted in immature alveoli [26]. From our knowledge, no previous research was done on postnatal Aluminum chloride affection of rat lung. Therefore, we will compare our results with adult rat lung. In aluminum chloride exposed rats at age 14 PND (H&E) stained sections show rat lung in the saccular stage of development. The air saccules were lined largely by squamous I pneumocytes and the II pneumocytes were interspersed singly among I pneumocytes. These findings agreed with Zhuang T, et al. (2010) who reported that bronchopulmonary dysplasia (BPD) remains a major cause for morbidity [27]. Aluminum chloride exposed rats at 21 day postnatal showed diffuse affection. Alveoli were seen collapsed in many areas with thickening of the interalveolar septa. In addition, some air passages filled with vacuolated acidophilic exudate could be detected. Some alveoli containing desquamated cells and other alveoli are interconnected. Cellular proliferation especially in pneumocytes II was seen. In addition, some pneumocytes II cells were seen extruded in alveolar lumen. Extravasations of RBCs and hemorrhage were also seen in some sections. This agreed with Wu L, et al. (2011) who reported proliferation of pneumocytes II with pale vacuolated cytoplasm [28]. Buraimoh AA, et al. (2013) as well observed blood vessels engorged with blood in aluminum subjected rats [9].

On light microscopic examination, the treated sections of the lung showed some histological changes that were at variance with those obtained in control. There was evidence of increased number of neutrophils and macrophages within the airspace, airway and blood vessels in Aluminum chloride resaved newborn pups compared with control section. Tian S, et al. (2009) stated that the present lesions in the lungs were not restricted on the vascular congestion but were associated with numerous areas of bronchopneumonia characterized by an excess of bronchiolar, peribronchiolar and alveolar infiltrations of mononuclear cells [29].

Al has been reported to cause oxidative stress of reduced glutathione [30]. Al Kahtani MA (2010) suggested that aluminum was able to induce oxidative stress in tissues which is described by EL-Dermerdash FM (2004) who stated that aluminum chloride generates reactive oxygen [31,32]. Buraimoh AA, et al. (2013) suggested that AlCl (Aluminum Chloride) detrimental effects on the histology of the lungs [9]. With an increase of malondialdehyde, hydrogen peroxide, and protein carbonyls levels [33-35]. Aluminum chloride exposed rats treated with Omega 3 at 14 and 21 days post-natal by (H&E) stain, showing a marked improvement in the histological pattern of the lung

Conclusion

The results of the study revealed that aluminum chloride-induced histological and immunohistochemical abnormalities in the lung of postnatal albino rats. Omega 3 improved the changes associated with Aluminum chloride administration. This study supports the usage of Omega 3 as protective against the toxic effects of Aluminum chloride.

Recommendations

According to the results, we recommend a reduction in the rate of exposure to aluminum chloride as much as possible. Trying to find a substitute for aluminum in the treatment of drinking water. Reducing the rate of occupational exposure of workers to aluminum compounds in different industries. The use of O3 compounds to reduce the toxic effects caused by exposure to aluminum chloride.

References

1. Baxter R, Hastings N, Law A, Glass EJ (2008) A rapid and robust sequence-based genotyping method for BoLA-DRB3 alleles in large numbers of heterozygous cattle. Anim Genet 39: 561-563.https://doi.org/10.1111/j.1365-2052.2008.01757.x
2. Krewski D, Yokel RA, Nieboer E, Borchelt D, Cohen J, et al. (2007) Human health risk assessment for aluminium, aluminium oxide, and aluminium hydroxide. J Toxicol Environ Health B Crit Rev 10: 1-269.https://doi.org/10.1080/10937400701597766
3. World Health Organization (1978) Introduction, ALMA-ATA-Primary Health Care. The International Conference on Primary Health Care, Switzerland.
4. Caron MF, White CM (2001) Evaluation of the antihyperlipidemic properties of dietary supplements. Pharmacotherapy 21: 481-487.https://doi.org/10.1592/phco.21.5.481.34499
5. Adkins Y, Kelley DS (2010) Mechanisms underlying the cardioprotective effects of omega-3 polyunsaturated fatty acids. J Nutr Biochem 21: 781-792.https://doi.org/10.1016/j.jnutbio.2009.12.004
6. Riihimäki V, Aitio A (2012) Occupational exposure to aluminum and its biomonitoring in perspective. Crit Rev Toxicol 42: 827-853.https://doi.org/10.3109/10408444.2012.725027
7. Laudy JA, Wladimiroff JW (2000) The fetal lung 1: developmental aspects. Ultrasound Obstet Gynecol 16: 284-290.https://doi.org/10.1046/j.1469-0705.2000.00228.x
8. Joshi S, Kotecha S (2007) Lung growth and development. Early Hum Dev 83: 789-794. https://doi.org/10.1016/j.earlhumdev.2007.09.007
9. Schittny JC, Burri PH (2007) Development and growth of the lung. Ann Rev Cell Dev Biol 139: 111-124.
10. Buraimoh AA, Ojo SA (2013) Effects of aluminium chloride exposure on the histology of lungs of wistar rats. J Appl Pharm 3: 18.https://doi.org/10.7324/JAPS.2013.30121
11. Koyuturk M, Yanardag R, Bolkent S, Tunali S (2007) The potential role of combined anti-oxidants against cadmium toxicity on liver of rats. Toxicol Ind Health 23: 393-401. https://doi.org/10.1177/0748233707081907
12. Ghorbel I, Elwej A, Chaabane M, Jamoussi K, Mnif H, et al. (2017) Selenium alleviates oxidative stress and lung damage induced by aluminum chloride in adult rats: biochemical and histological approach. Biol Trace Elem Res 176: 181-191.https://doi.org/10.1007/s12011-016-0818-9
13. Bancroft JD, Gamble M (2008) Theory and practice of histological techniques. (6th edtn), Elsevier Health Sciences, London, United Kingdom.
14. Yamada T, Suzuki E, Gejyo F, Ushiki T (2002) Developmental changes in the structure of the rat fetal lung, with special reference to the airway smooth muscle and vasculature. Arch Histol Cytol 65: 55-69.https://doi.org/10.1679/aohc.65.55
15. Dean AG, Sullivan KM, Zubieta J, Delhumeau C (2000) Epi Info 2000: a database, and statistics program for public health professionals for use on Windows 95, 98, and NT computers. Centers for Disease Control and Prevention, Unites States.
16. Ali HA, Afifi M, Abdelazim AM, Mosleh YY (2014) Quercetin and omega 3 ameliorate oxidative stress induced by aluminium chloride in the brain. J Mol Neurosci 53: 654-660.https://doi.org/10.1007/s12031-014-0232-8
17. Kamal I, Kamal H (2013) Effects of aluminum on rat cerebellar cortex and the possible protective role of nigella sativa. Egypt J Histol 36: 979-990.https://doi.org/10.1097/01.EHX.0000440828.86537.e7
18. Bolle I, Eder G, Takenaka S, Ganguly K, Karrasch S, et al. (2007) Postnatal lung function in the developing rat. J Appl Physiol 104: 1167-1176.https://doi.org/10.1152/japplphysiol.00587.2007
19. Ross MH, Pawlina W (2009) Histology-A text and Atlas. (5th edtn), Lippincott Williams and Wilkins, United States.
20. Tomashefski JF, Farver CF (2008) Dail and Hammer's Pulmonary Pathology. (3th edtn), Springer, United States.
21. Prodhan P, Kinane TB (2002) Developmental paradigms in terminal lung development. Bioessays 24: 1052-1059.https://doi.org/10.1002/bies.10177
22. Roth-Kleiner M, Post M (2005) Similarities and dissimilarities of branching and septation during lung development. Pediatr Pulmonol 40: 113-134.https://doi.org/10.1002/ppul.20252
23. Ahmed RR, Mazher K (2009) Histological, histochemical and biochemical changes in the liver, kidney, lung and spleen under the effect of repetitive hyperthermia in rat neonates. Iran J Cancer Prev 2: 91-101.

24. Ibáñez-Vea M, Zuazo M, Gato M, Arasanz H, Fernández-Hinojal G, et al. (2018) Myeloid-derived suppressor cells in the tumor microenvironment: current knowledge and future perspectives. Arch Immunol Ther Exp 66: 113-123.https://doi.org/10.1007/s00005-017-0492-4

25. Prokopakis E, Vardouniotis A, Kawauchi H, Scadding G, Georgalas C, et al. (2013): The pathophysiology of the hygiene hypothesis. Int J Pediatr Otorhinolaryngol 77: 1065-1071.https://doi.org/10.1016/j.ijporl.2013.04.036

26. Warburton D, Bellusci S, De Langhe S, Del Moral PM, Fleury V, et al.(2005) Molecular mechanisms of early lung specification and branching morphogenesis. Pediatr Res 57: 26R-37R.https://doi.org/10.1203/01.PDR.0000159570.01327.ED

27. Zhuang T, Zhang M, Zhang H, Dennery PA, Lin QS (2010) Disrupted postnatal lung development in heme oxygenase-1 deficient mice. Respir Res 11: 142.https://doi.org/10.1186/1465-9921-11-142

28. Wu L, Wang G, Qu P, Yan C, Du H (2011) Over expression of dominant negative peroxisome proliferator-activated receptor-γ (PPARγ) in alveolar type II epithelial cells causes inflammation and T-cell suppression in the lung. Am J Pathol 178: 2191-2204.https://doi.org/10.1016/j.ajpath.2011.01.046

29. Tian S, Jiang P, Ning P, Su Y (2009) Enhanced adsorption removal of phosphate from water by mixed lanthanum\aluminum pillared montmorillonite. Chem Eng 151: 141-148.https://doi.org/10.1016/j.cej.2009.02.006

30. Gonzalez MA, del Lujan Alvarez M, Pisani GB, Bernal CA, Roma MG, et al. (2007) Involvement of oxidative stress in the impairment in biliary secretory function induced by intraperitoneal administration of aluminum to rats. Biol Trace Elem Res 116: 329-348.https://doi.org/10.1007/BF02698017

31. Al-Kahtani MA (2010) Renal damage mediated by oxidative stress in mice treated with aluminium chloride: protective effects of taurine. J Biol Sci 10: 584-595.https://doi.org/10.3923/jbs.2010.584.595

32. El-Demerdash FM (2004) Antioxidant effect of vitamin E and seleniumon lipid peroxidation, enzyme activities and biochemical parameters in rats exposed to aluminium. J Trace Elem Med Biol 18: 113-121.https://doi.org/10.1016/j.jtemb.2004.04.001

33. Stein DJ, Hollander E, Rothbaum BO (2009) Textbook of anxiety disorders. (2nd edtn), American Psychiatric Publishing, United Kingdom.

34. Kiernan JA (2000) Histological and Histochemical Methods: Theory and Practice. (3rd edtn), Butterworth Heinemann, United Kingdom.

35. Mitchell JJ, Reynolds SE, Leslie KO, Low RB, Woodcock-Mitchell J (1990) Smooth muscle cell markers in developing rat lung. Am J Respir Cell Mol Biol 3: 515-523. https://doi.org/10.1165/ajrcmb/3.6.515